



Neogene and Quaternary dikes and related joints as conduits for recent juvenile degassing: case studies from the seismically active region of NW-Bohemia, Czech Republic

J. Heinicke¹ · H. Woith² · C. Alexandrakis-Zieger¹ · S. Buske¹ · R. K  ppler¹ · O. Krentz¹ · P. Menzel¹

Received: 14 October 2022 / Accepted: 28 April 2023 / Published online: 26 May 2023
  The Author(s) 2023

Abstract

The contemporary occurrence of juvenile gas emissions at springs or mofettes in active volcanic areas can be observed worldwide. This correlation is less frequent in areas with dormant or post-volcanic activity. The NW-Bohemia/Vogtland region located at the Eger rift zone (Czech Republic) provides an intriguing example of this correlation between numerous Neogene-aged post-volcanism locations and juvenile fluid emission sites. Newly discovered dikes and diatremes are located close to vents with the highest helium isotope ratios ($^3\text{He}/^4\text{He}$) of about $6 R_a$. Our results lend support to the hypothesis that feeder dikes and their fractured wall rocks should be considered the predominant conduits for the continuous upwelling of juvenile fluids. Moreover, 77% of the CO_2 gas emission sites are located close to dikes or diatremes, i.e., within a distance of 4 km. Our studies reveal a spatial dependence of the R_a values at the spring sites with the estimated distances to the basaltic bodies. The results confirm the negative trend known from the literature. That is, R_a values decrease with increasing distance from the feeder dikes.

Keywords Neogene volcanism · Feeder dikes · Juvenile fluids · Mineral springs · Helium isotope

Introduction

Emission of mantle-derived volatiles (e.g., CO_2) can be observed worldwide at mineral springs and mofettes. Inter-connected fracture systems in the crust are the most probable pathways in non-volcanic areas (Caracausi and Sulli 2019; Chiodini et al. 2010; Kennedy and van Soest 2007; Kulon-goski et al. 2013; Tamburello et al. 2018). Ascent paths have also been linked to diatremes and dikes which represent a direct link between magmatic reservoirs at depth and the uppermost crust or surface (Dahm et al. 2020; Fischer 2008; Griesshaber et al. 1992; Hunt et al. 2017; Perez et al. 2011; Sano et al. 1984; Sorey et al. 1998). Extensional tectonic

processes due to the regional stress field are important factors for the activation and reactivation of dike propagation as well as the ascent of juvenile fluids in the crust (Gudmundsson et al. 2022; Tamburello et al. 2018). Examples of juvenile fluid degassing in the vicinity of dormant volcanos have been reported worldwide at locations such as Mt. Vulture (Caracausi et al. 2015), in the Carpathian-Pannonian Region (Kis et al. 2017), and in Siberia (Tang et al. 2013). During the Cenozoic, intraplate alkaline volcanism formed the Central European Volcanic Province. This province is associated with a WSW-ENE trending Cenozoic rift system which extends from the Massif Central in France through the Eifel in Germany to the Eger Rift in Czech Republic and Lusatia in Poland (Fig. 1a) (B  chner et al. 2015; Ulrych et al. 2011). Today, emission of juvenile fluids rich in CO_2 and with elevated ^3He contents is common at mineral springs or mofettes within this province (Br  uer et al. 2013, 2017; Carl   1958, 1975; Pearce et al. 2004). Carl   (1975) published a comprehensive collection of fluid emission sites across this province, collating fluid chemistry and the relation of emission sites to their hydrogeological sources and the geological basement. Other locations of CO_2 emission close to Neogene diatremes are known in the Rhine graben

Editorial Responsibility: J. Xu

✉ J. Heinicke
jens.heinicke@extern.tu-freiberg.de

¹ Institute of Geophysics and Geoinformatics, TU Bergakademie Freiberg, Gustav-Zeuner-Str. 12, 09599 Freiberg, Germany

² GFZ German Research Centre for Geosciences, 14473 Potsdam, Germany

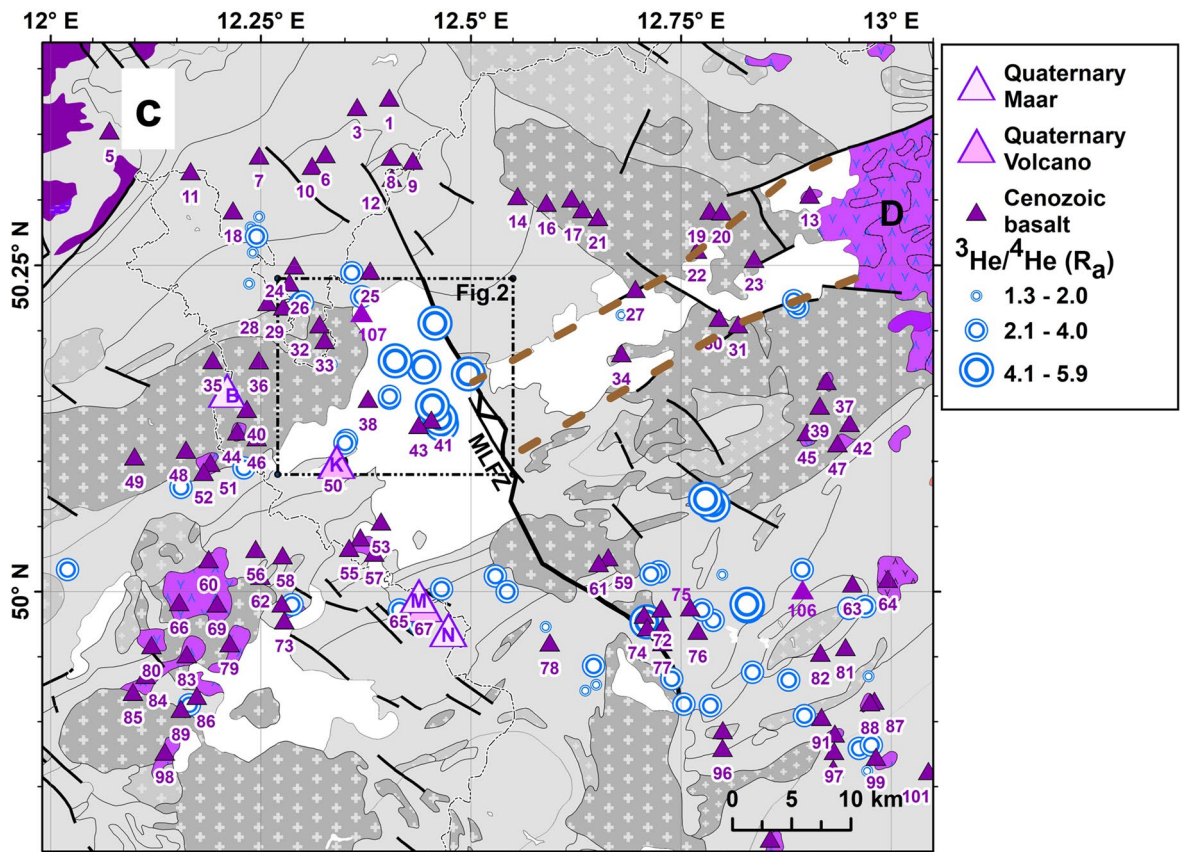
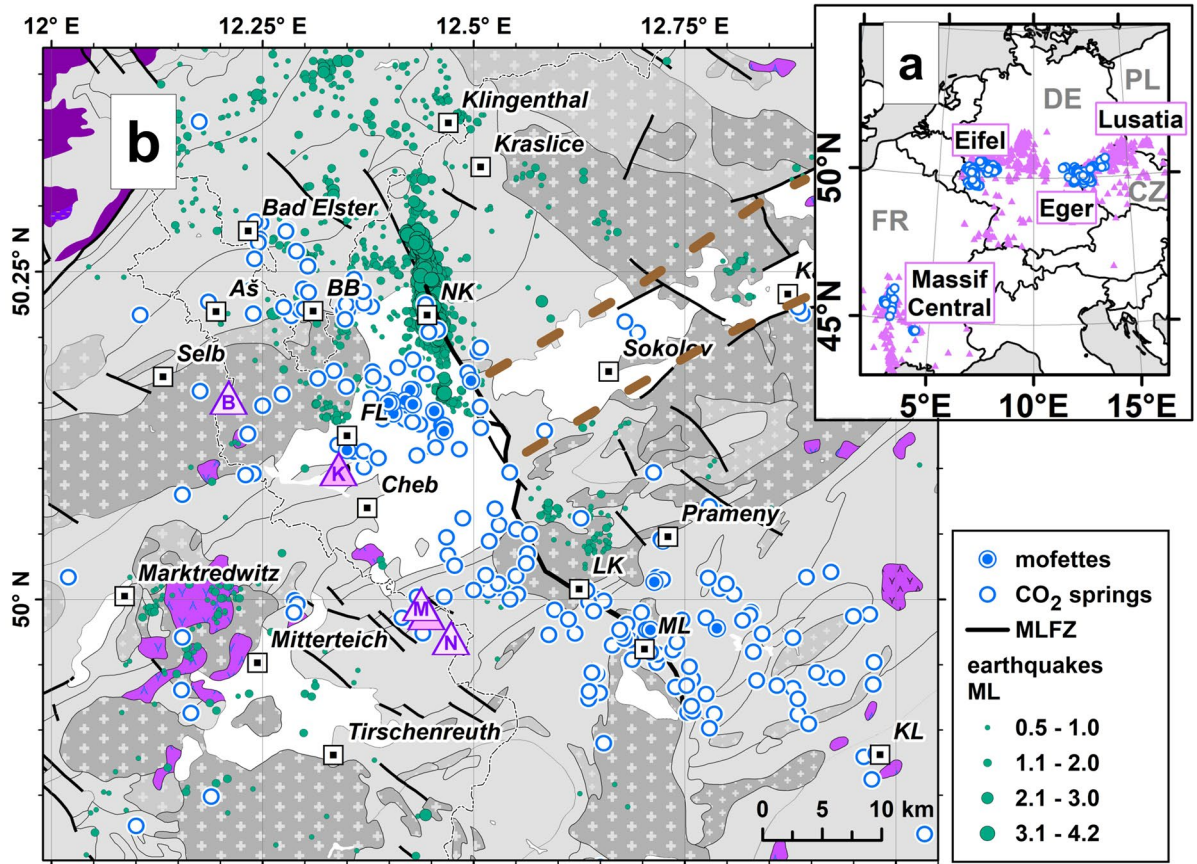


Fig. 1 **a** Simplified map of the Central European Volcanic Province. **b** Simplified geological map of the Regensburg–Leipzig zone (RLZ) between 12° and 13°E of the NW-Bohemia/Vogtland region with the distribution of earthquake epicenters and juvenile fluid emission sites corresponding to mofettes and CO₂-containing mineral springs following Heinicke and Woith (2022). Gray: metasediments, white: Cenozoic sediments, grey with white crosses: granitic basement, and purple: alkaline volcanic rocks. Map source: BGR Hannover. **c** Geology with location of basaltic structures mapped by Cháb et al. (2007), Ulrych et al. (2011, 2016), Emmert et al. (2007), and Hoth et al. (1981) as well as those located by this study (purple numbered triangles): M: Mýtina maar (covered the Železná hůrka volcano); N: Bad Neualbenreuth maar; K: Komorní hůrka; B: Liba maar; D: Doupovské Hory volcano. Black lines: fault zones; MLFZ: Mariánské Lázně fault zone; brown dashed line: Eger Rift zone; BB: Bad Brambach; NK: Nový Kostel; FL: Františkovy Lázně; K: Karlovy Vary; LK: Lázně Kynžvart; ML: Mariánské Lázně; KL: Konstantinovy Lázně

(Clauser et al. 2002; Griesshaber et al. 1992), Bad Urach (Carlé 1958), and the Black Forest (SW-Germany). Here, mineral springs containing CO₂ are active, for example, near the village Oppenau as at Bad Antogastand Bad Griesbach (Stober 1995). Mineral springs with mantle-derived CO₂ are also active in the western Eger Rift and around the Cheb basin (Czech Republic, NW Bohemia, Fig. 1b) (Bräuer et al. 2018; Weinlich et al. 1999). Anomalously high ³He/⁴He ratios (R_a) of up to 6 R_a at these springs suggests a link to recent volcanism or magmatic unrest (Bräuer et al. 2014). However, an open question is the transport pathway for the ascending juvenile fluids toward the surface.

For the NW-Bohemia/Vogtland region, Babuška and Plomková (2008) suggested that microplate boundaries act as conduits for ascent of juvenile fluids from the lithospheric mantle. Here, we explore whether diatremes and dikes associated with the Cenozoic volcanic activity in the NW-Bohemia/Vogtland region could provide a direct link to the asthenosphere to feed the mantle-derived CO₂ emissions. To do this, we combine stratigraphic analyses with geomagnetic survey data. This allows us to locate sub-surface basaltic bodies and assess their influence on the present distribution of degassing sites.

Geological setting, the occurrence of juvenile fluids

Tectonic

The geological basement of the NW-Bohemian massif is a part of the Saxo-Thuringian zone and comprises a complex nappe stack of strongly foliated metasedimentary and meta-igneous rocks of varying metamorphic grade (Kroner et al. 2007). Intrusion of post-Variscan granitic plutons in the NW-Bohemia/Vogtland region, the Fichtelgebirge/Smrčiny granite, comprises an older (320 Ma) complex and a younger (290–280 Ma) complex (Hecht et al. 1997). The most

prominent tectonic structure of the NW-Bohemian/Vogtland region is the Regensburg–Leipzig Zone (RLZ) (Fig. 1b), which is about 700 km long and 40 km wide (Bankwitz et al. 2003; Pohl et al. 2006; Sonnabend 2022). The zone is composed of major N-S structures and en-echelon segments which are seismically active (Dahm et al. 2018; Fischer et al. 2014; Korn et al. 2008). A second major tectonic element is the ENE-WSW striking Cenozoic Eger Rift (Fig. 1b). This rift zone is part of the Central European Volcanic Province (Fig. 1a).

The late Variscan, Oligocene/pre-Neogene, and the Pliocene were periods of tectonic activity along the eastern marginal fault of the Cheb basin, a continuation of the active shear zone of the NNW–SSE trending Mariánské Lázně fault zone (MLFZ, Fig. 1c) (Peterek et al. 2011; Pitra et al. 1999; Špičáková et al. 2000). During the late Oligocene and Pliocene, subsidence of the Cheb basin occurred, where its deepest part is 300 m deep, which is located at the eastern margin of the basin. Sedimentation in the basin began in the early Miocene and continued through the Pliocene and Quaternary (Pešek et al. 2014; Špičáková et al. 2000).

According to Ulrych et al. (2011), Cenozoic volcanic activity began during the pre-rift period (79–49 Ma) along the Eger Rift due to the Erzgebirge uplift and rift zone subsidence (Abratis et al. 2009; Ackerman et al. 2013, 2015; Brandl et al. 2015; Büchner et al. 2015; Cajz et al. 2009; Chadima et al. 2009). The second volcanic period occurred between 42 and 16 Ma, with a late-rift phase occurring during 16–0.3 Ma. In the late Oligocene–early Miocene epoch, numerous eruptions fed by basaltic magmas can be associated with small dikes or diatremes in the Eger Rift zone, where the Doupovec stratovolcano is also located (Fig. 1c). Volcanism was probably linked to and influenced by the magmatic activity in the mantle-crustal transition (Hrubcová et al. 2017) and the NW–SE trending regional stress field (Heidbach et al. 2018; Korn et al. 2008). A few of these volcanic structures are still visible (e.g., Podhorní vrch #75, Pechbrunn #82, Wartberg #35, Fig. 1c), but others are today covered by sediments or have been eroded. Our study focuses on these volcanic structures, their spatial distribution, and their relation to the juvenile fluid emission sites.

Seismicity

A high rate of seismicity has been recorded in this region and is located along the N-S trending lineament, the RLZ (Dahm et al. 2018; Fischer et al. 2014; Horálek et al. 1996; Sonnabend 2022). These earthquakes and earthquake swarms with numerous micro-earthquakes occur frequently with magnitudes up to $M_L = 4.6$ being recorded in 1985/86. The epicenters of the most active earthquake swarm clusters are located around the village of Nový Kostel (Fig. 1b). Fischer et al. (2014) give a comprehensive description of the earthquake

swarm activity. The reasons for the earthquake swarm activity of the region are still under investigation (Heinicke et al. 2022; Vavryčuk et al. 2021; Vavryčuk and Hrubcová 2017). The main causes could be the regional stress field (Heidbach et al. 2018), the magmatic underplating (Fischer et al. 2014; Hrubcová et al. 2017), and a possible influence of magmatic unrest below the major hypocenter of Nový Kostel (Dahm et al. 2008; Fischer et al. 2014; Špičák et al. 1999).

Juvenile fluids

The hydrogeological situation of the Cheb basin and the Vogtland area is described in Burda and Baburek (1998), Egerter et al. (1984), Storch (1998), and Springorum (2000). The numerous mineral springs are fed by subsurface water with recharge in the basin shoulder areas. Mixing with juvenile CO₂ in shallow aquifers reduces the pH and increases the solubility of minerals from the host rocks, which are mostly basin sediment layers. This mineralized water feeds spas such as Františkovy Lázně, Mariánské Lázně, Bad Brambach, Bad Elster, and Karlovy Vary (Fig. 1b). Springs are also located on the western edge of the Eger Rift zone (Weinlich et al. 2003) and across the eastern part of the rift zone. All such springs show signs of mantle-derived fluids, as is apparent from the $\delta^{13}\text{C}$ values of the CO₂ phase of the water (Dupalová et al. 2012; Geissler et al. 2005; Weinlich et al. 2003).

The widespread distribution of mantle-derived CO₂ at mineral springs and mofettes is given in Fig. 1b, and about 300 mineral springs or mofettes are registered in our database (Heinicke and Woith 2022). This database is built on our own field work, published data (Bälz 1908; Bräuer et al. 2018; Dietl 1942; Geissler et al. 2005; Jahnel 1937; Springorum 2000; Weinlich et al. 1999, 2003) and web-based sources (e.g., www.estudanky.eu) (Fig. 1b). Only a few have been sampled and analyzed for their chemical contents (Egerter et al. 1984; Storch 1998), but the isotopic signature of CO₂ emissions analyzed by Weinlich et al. (1999) and Geissler et al. (2005) indicates a magmatic origin with $\delta^{13}\text{C}$ values of -4.3 to -2 $\delta^{13}\text{C}_{\text{PDB}}$ (CO₂) (‰). In addition, the ³He mantle contribution is in the range of subcontinental mantle fluids (Gautheron et al. 2005), with R/R_a (atmospherically corrected ³He/⁴He ratios) of up to 6 R_a (Bräuer et al. 2008, 2018; Geissler et al. 2005; Weinlich et al. 1999, 2003). Available ³He/⁴He ratios and $\delta^{13}\text{C}$ data and additional analysis by the INGV (Istituto Nazionale di Geofisica e Vulcanologia, Palermo, Italy) are compiled as Supplementary Information S2. The spatial distribution of the gas emission sites is concentrated along a NW–SE trending zone that crosses the Eger Rift (Fig. 1b) (Heinicke and Woith 2022). Figure 1c shows the distribution of the R_a values based on the supplementary information list S2.

Methods

Stratigraphic analysis

We separate the areas of metasedimentary basement from the granitic basement in the Cheb basin analyzing the local basement and its stratigraphy using more than 100 drill sites completed by the Czech Geological Survey (ČGS) in Praha (Czech Republic) (Fig. 2). Drill site locations were used to map the distribution of alkaline magmatic rocks above the basement (Fig. 2). The ČGS boreholes vary in depth between 100 and 300 m, with one deep borehole # 627479 having a depth of about 1200 m. Thus, our assessment applies to this depth range.

Magnetic surveys

The selection of survey areas was based on the borehole stratigraphy plus the Saxonian regional geomagnetic map of Börner and Käppler (2019). Other sites were surveyed on the assumption that mapped volcanic structures should be associated with gas emission centers whose R_a values are increased, e.g., greater than 2.

The magnetic survey was performed using proton magnetometer of the type G856 (*Geometrics*) and PMG-2 (*Satis-Geo*). We used also an Overhausen magnetometer GSM-19W (*GEM Systems*). All sensors give intensity T of Earth's magnetic field with an absolute accuracy of ≤ 0.1 nT. Diurnal variations were continuously recorded (1-min interval) at a base station near the village of Kopanina (Fig. 3). All measurements were referenced to this base station with a magnetic anomaly value $dT=0$ nT. The accuracy of the survey data dT is around ± 1 nT. The profiles were selected as an irregular grid depending on topographic reasons. The distance of the measurement points at the profiles was about 20 m.

Further, we created a 3D susceptibility model for one location ("43") using the interactive potential field modeling software IGMAS+ (Anikiev et al. 2020; Götze and Lahmeyer 1988) to achieve a geometric image of the volcanic structure. Three relevant susceptibility bodies in the model are used with their assumed susceptibility values: metasediments: $0.2 \cdot 10^{-3}$ (SI); basalt: 0.025 (SI) and the Cenozoic and Quaternary sediment cover with a zero susceptibility. The model also includes the borehole data of #102609 with a basalt layer of about 26 m thickness.

Results

We find widespread association of volcanoclastics, basalts, or tephra layers with mostly hidden diatremes or dikes (Fig. 1c). The distribution of the diatremes and dikes, in

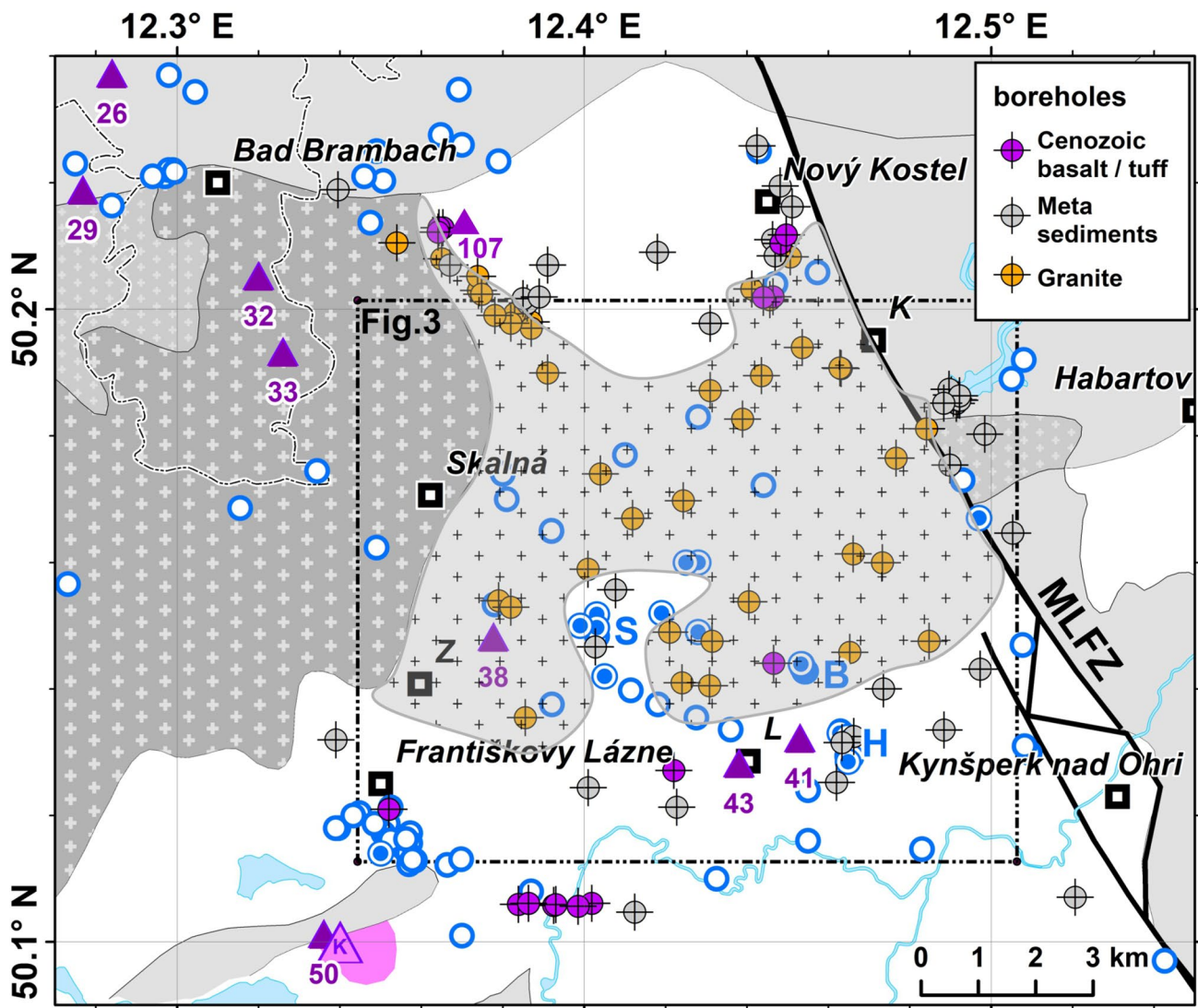


Fig. 2 The Cheb basin and surrounding areas with the geology and CO₂ gas emission sites (blue circles, from Heinicke and Woith (2022)). The stratigraphy based on the borehole sites of the Czech Geological Survey (ČGS; www.geology.cz) is described in the leg-

end. Black crosses on gray background show the covered granitic basement following Mlčoch and Skácelová (2009). Zones of gas emission at springs or mofettes are marked as Soos (S), Hartoušov (H), and Bublák (B); villages: L: Lesina; K: Kopanina; Z: Žirovice

particular of the Neogene volcanism, was underrepresented in the literature (e.g., Fischer et al. 2014; Geissler et al. 2005). However, these structures could act as pathways for ascending juvenile fluids.

Stratigraphic analysis

The analysis of borehole documents revealed deposits relating to alkaline volcanism ranging from thin sheets of volcanoclastics of a few centimeters thick (e.g., S of Nový Kostel, Fig. 2) to basaltic layers of up to 30 m in thickness (e.g., at boreholes #102607, Fig. 5 and SE of FL, Fig. 3). All deposits are located on top of the

Variscan basement. These volcanic deposits are thus late Oligocene to early Miocene. Analysis of the tectonosedimentary evolution of the Cheb basin has been carried out by Špičáková et al. (2000), who found that the main volcanic phase can be dated to 30–21 Ma. One tuff deposit at a borehole S of Nový Kostel/Lesna (borehole #548887) was dated to 21.1 Ma with paleomagnetic investigations (Bucha et al. 1990), but according to Špičáková et al. (2000), this age is only an approximation. However, this age of around 21 Ma is comparable to age determinations for diatremes located about 40 km to the west in NE-Bavaria (Rohrmüller et al. 2005) and in southern Vogtland (Abratis et al. 2009).

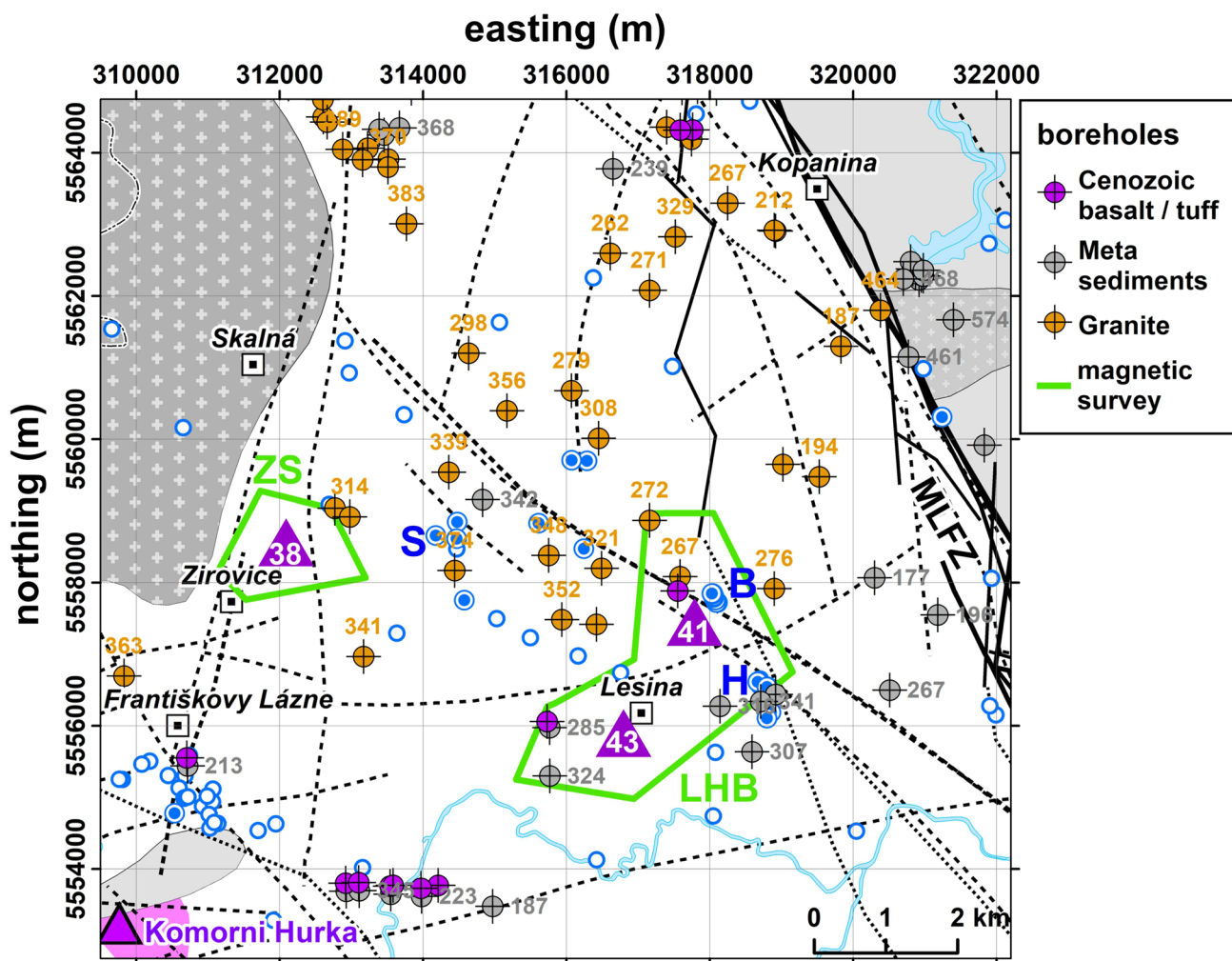


Fig. 3 Part of the Cheb basin with the areas of the magnetic survey at Žirovice-Soos (ZS) and Lesina-Hartoušov-Bublák (LHB). The discovered diatremes and dikes (pink triangles: 38, 41, and 43) are close to the gas escape centers of Soos (S), Hartoušov (H), and Vackovec/Bublák (B), respectively. Solid lines indicate major faults, and dashed

lines are local fault zones according to the geological map 1: 50,000, Prague: Česká geologická služba [cit. 2018–03-21]. The coordinate system has been changed to UTM 33N for a better display of the survey results on a smaller scale. Numbers next to the boreholes indicate the top of the respective geological unit in m above sea level (a.s.l.)

Magnetic survey

An increased magnetic total intensity T of Earth’s magnetic field indicates a large amount of magnetic rocks (e.g., basalt) or high contents of magnetic minerals in the subsurface. This increased magnetic field could generate a positive or negative anomaly according to the global orientation of the Earth’s magnetic field during the cooling process of the magma, as observed in our measurements. Different diatreme structures along the eastern Cenozoic rift system show increased magnetic field values of the anomalies between 80 and 1300 nT (Flechsigt et al. 2015; Lindner et al. 2006; Mrlina et al. 2009; Skácelová et al. 2012).

The results of the magnetic surveys allow us to distinguish areas with and without elevated magnetic total fields used to interpret the locations of possible magmatic

structures based on their elevated magnetic signature. The magnetic susceptibility of the alkaline magmatic rocks in this region has been found to be three to four orders of magnitude greater than that of the local sediment cover, granite, or metasediments (Mrlina et al. 2007; Skácelová et al. 2012).

Our magnetic survey shows anomalies with amplitudes between -130 and $+2040$ nT compared with an accuracy of ± 1 nT. The distribution of the 17 areas of our magnetic survey is presented in the supplementary information list S1, map SM1, and Fig. 1c.

The locations of the most important areas for our studies, because they are new discovered volcanic structures and they are located close to strong gas emission zones, are indicated in Fig. 3. The area south of the city of Františkovy Lázně “FL” (Fig. 3) is an additional volcanic structure that can be associated with a Quaternary

volcano, the Komorni hůrka (Kammerbühl). This volcano represents the most recent magmatic activity of the “FL” area. A comprehensive magnetic survey of these structures was not possible due to the presence of the city. Evidence in borehole logs around the city confirms the distribution of basaltic and tephra layers to the southeast (boreholes, e.g., #565848) and to the north (Pešek et al. 2014). However, at Komorni hůrka, basaltic deposits and the emission of juvenile fluids at numerous springs support a possible link between the presence of diatremes and/or dikes and juvenile fluid emission.

Area “ZS” (“Žirovice- Soos”)

The area “ZS” is located NE of Žirovice, 1500 m west of the Soos park area (Fig. 3). It was first investigated by Dobeš et al. (1986) and was interpreted as a tectonic depression with volcanoclastics or with a coal seam formation. Our magnetic survey reveals a ring structure with a negative magnetic anomaly (−130 nT). The ring-like orientation of this anomaly (“38,” Fig. 4) hints at a basaltic body that probably was associated with a maar diatreme and a surrounding tephra ring (Lorenz 2007; White and Ross 2011). The surrounding volcanoclastics and tephra deposits have been partly eroded.

Ascending magma probably followed a N-S trending zone of fractured basement formed during the subsidence of the Cheb basin in the late Oligocene (Fig. 4). Further fracture zones could have been created during magma ascent and eruption around the feeder dike (Buck et al. 2005; Delaney et al. 1986; Gudmundsson and Loetveit 2005). The regional stress field (NW–SE) could keep these fractures open and allow fluid transport toward the surface. The high mantle helium content of 3.3 R_a (Bräuer et al. 2018) in the Soos emission area indicates a relatively short migration path in the upper crust which would reduce the R_a values due to the addition of radiogenic ^4He .

Area “LHB” (“Lesina-Hartoušov-Bublák”)

Area “LHB” is a magnetic anomaly of about 1.5 km * 3 km (Fig. 5). Massive basaltic and tephra layers can be found at two boreholes within the anomaly, confirming the presence of a volcanic structure at depth. At borehole #102607, a basaltic layer of about 30 m in thickness is located above the granitic basement at a depth of 134 m. At borehole #102609, there is a basaltic layer of 26 m in thickness at a depth of 111 m lying on the metasediment basement.

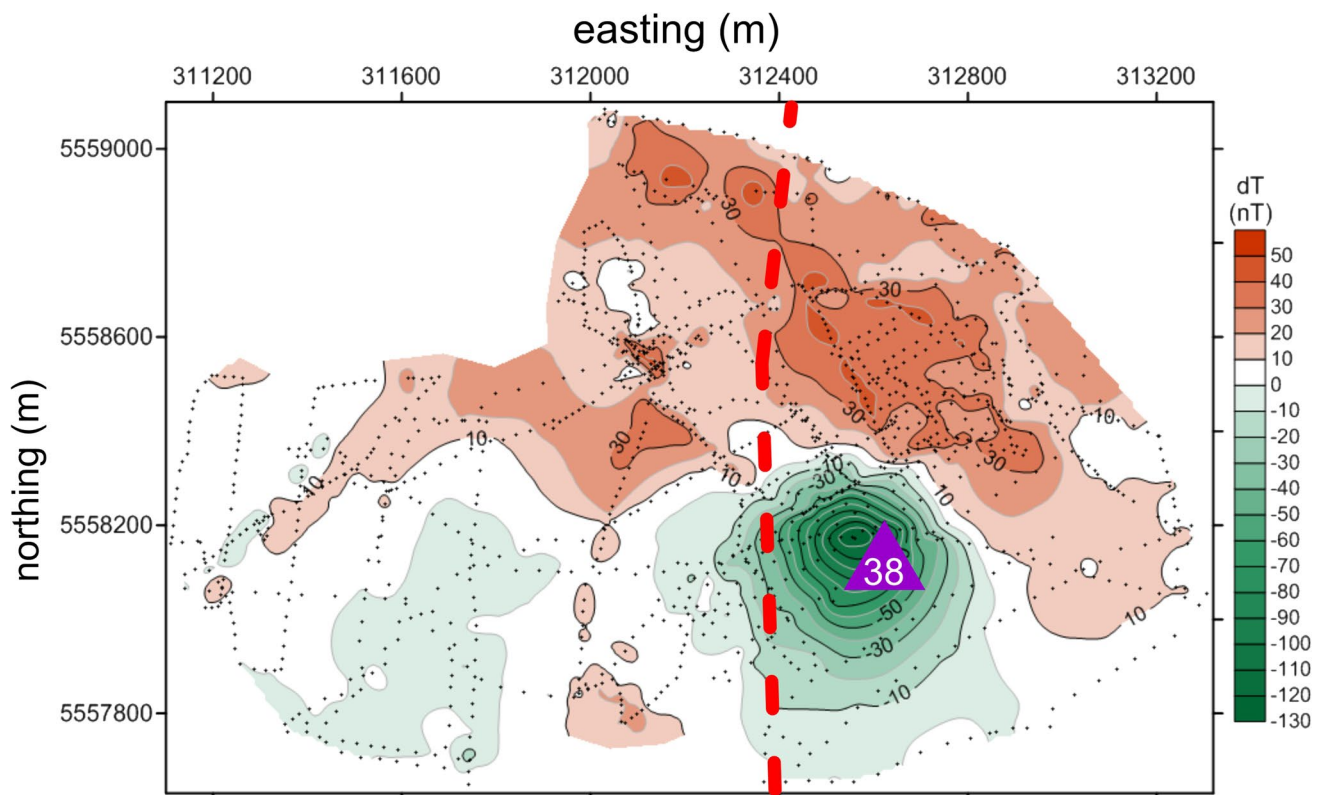


Fig. 4 Negative magnetic anomaly of the Žirovice maar diatreme, dT anomaly “38” The coordinates are in UTM 33N. Red dashed line: N-S trending fault zone taken from the ČGS geological 1:50.000 map; black points: measurement locations used for the magnetic survey

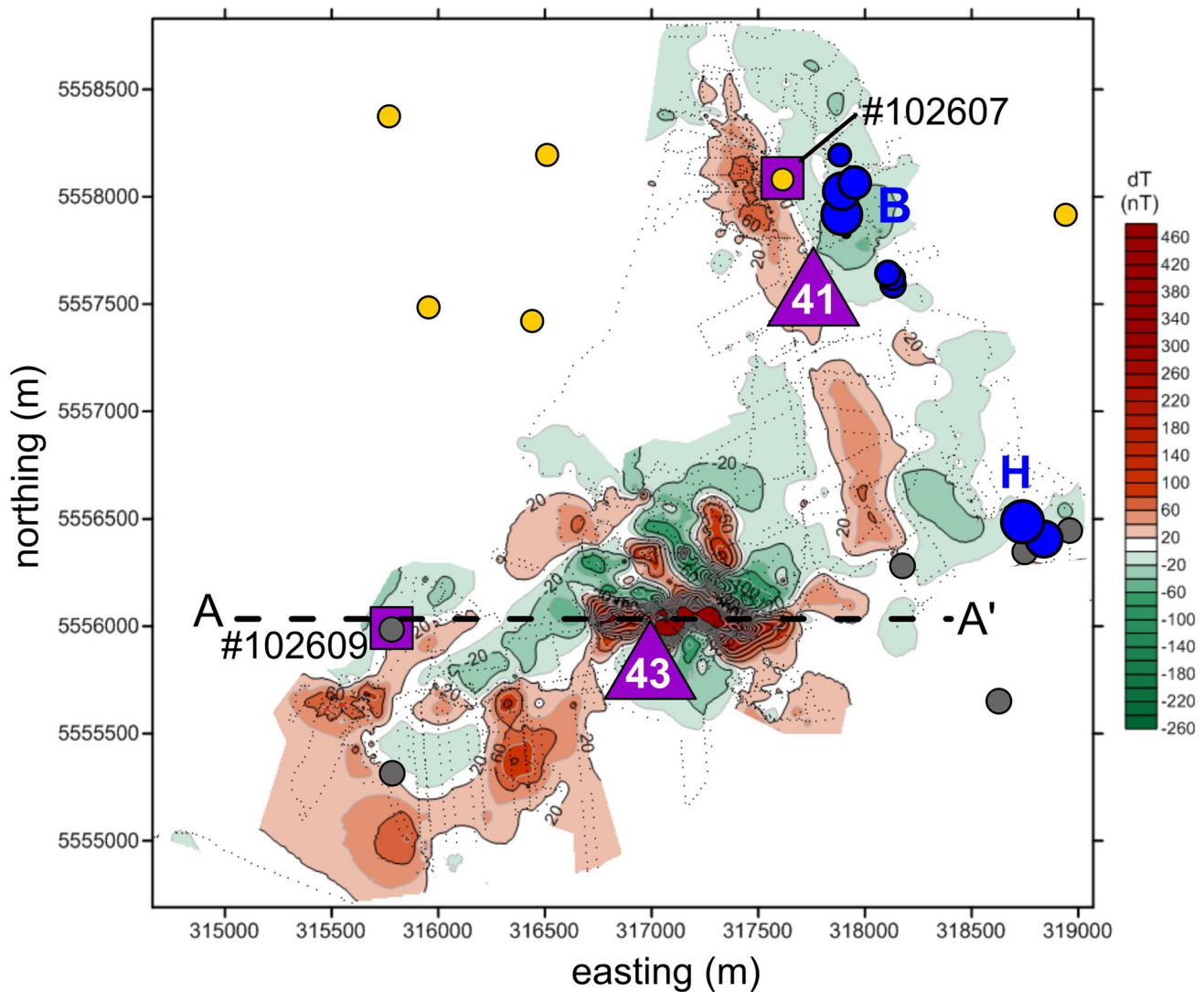


Fig. 5 Magnetic anomalies of the “LHB” area. Coordinates are in UTM 33N. The buried volcanic structures are indicated by the numbers “41” and “43.” Blue points: degassing centers of Hartoušov (H) and Bublák/Vackovec (B) (Kämpf et al. 2019); purple squares: drill

sites where basalt is found; deep yellow points: drill sites where only granitic basement is found; grey points: drill sites with metasediment basement; small black points: measurement points; black dashed lines A-A’: profile of the 3D modeling given in Fig. 7

The magnetic anomaly of “LHB” is divided in two parts (Fig. 5). The first (“43,” Fig. 5) has maximum values of dT of 800 nT and has an elongate form with an E-W extension of about 1 km. We consider this to be a dike, intruded along a tectonic weak zone as indicated in Fig. 6, which could be an extensional fault zone caused by rifting with a N-S oriented extension during the early Oligocene (Peterek et al. 2011; Ulrych et al. 2003).

The second part (“41,” Fig. 5) is a dT anomaly of about 100 nT and shows a NNW-SSE trend. We also interpret this as a dike intruded along a normal fault zone (red dashed line, Fig. 6). Vertical displacements of the granite and metasediment basement (Fig. 6) show a down throw of -80 m toward the ENE, consistent with the fault zone being associated

with subsidence of the Cheb basin. We suggest that this fault zone is probably responsible for the Oligocene/Neogene magma ascent, which formed additional fracture zones for the recent fluid supply that feed toward the mofettes of Bublák/Vackovec and Hartoušov, the two strongest gas emission zones of the Cheb basin.

Our 3D susceptibility model of the main anomaly “43” (Fig. 7) shows that the magnetic anomalies of LHB are associated with volcanic structures with thicknesses of 80–100 m, at a mean depth of 100–150 m (line A–A’, Fig. 7). The anomaly can thus be modeled as a basaltic body with an east–west extension of ~ 1000 m, a north–south extension of 100 m, a mean depth (below the current surface) of less than 25 m, and a thickness of at least 250 m.

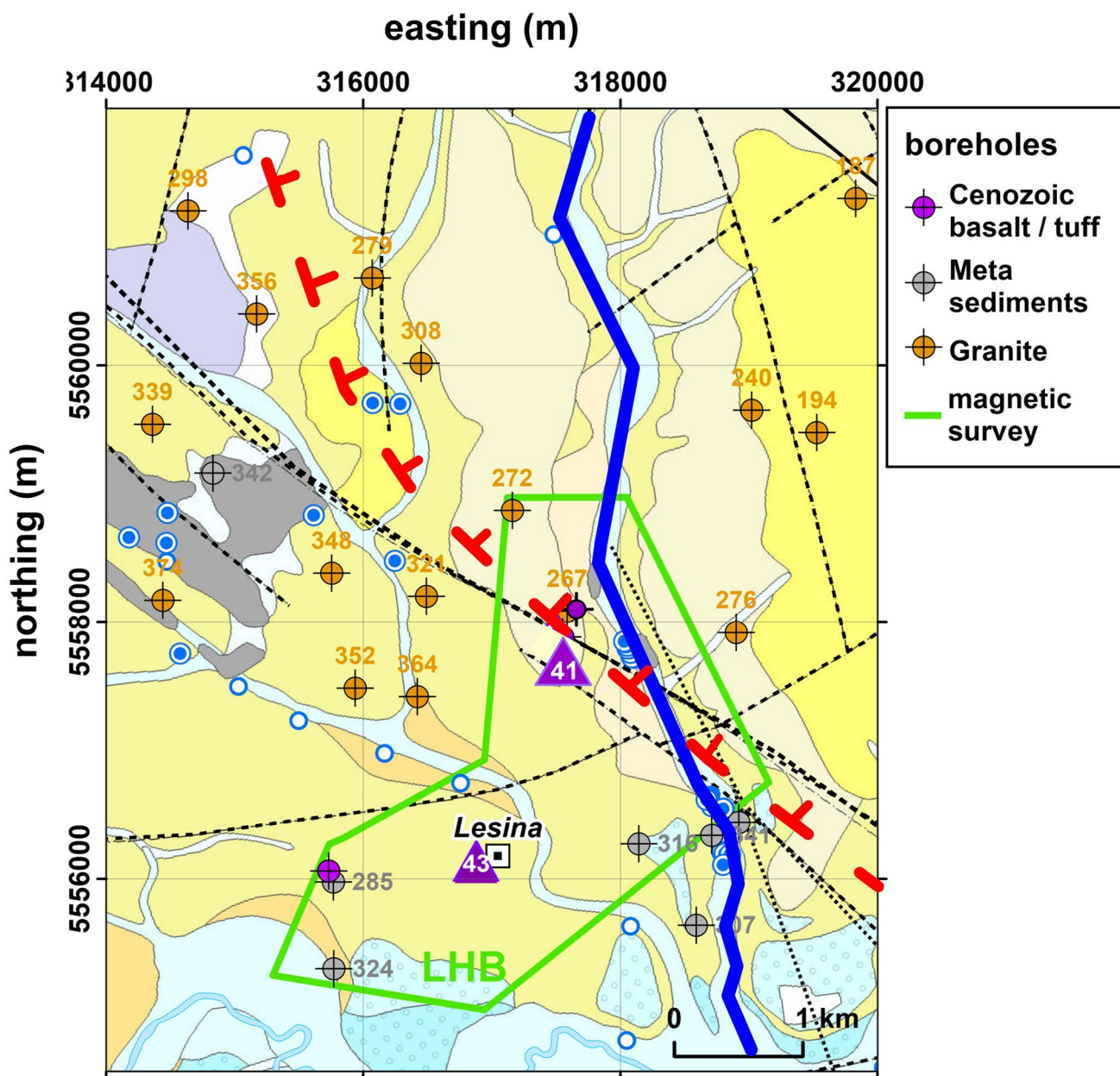


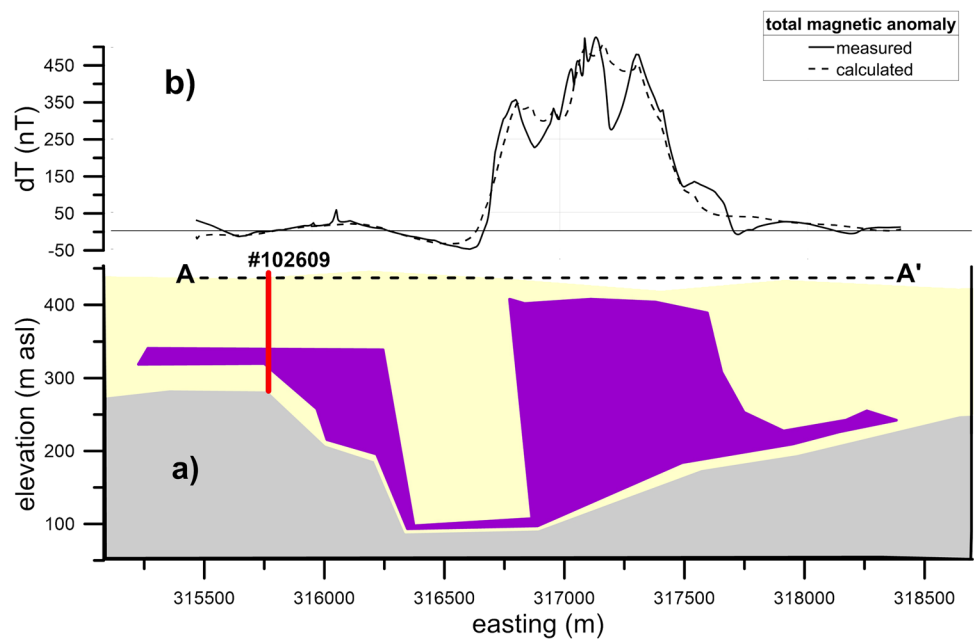
Fig. 6 Dikes “41” and “43” of “LHB” (purple triangles) aligned with two fault zones indicated by black dashed lines. Uppermost basement levels from the borehole stratigraphy are given in m a.s.l. Blue points: CO₂ emission sites; blue line: Plesna river; black dashed lines: tectonic faults from the ČGS 1:50.000 geological map. The red dashed

line indicates a possible normal fault related to the subsidence of the Cheb basin. This line is estimated following Špičáková et al. (2000) and Mičoch et al. (2009) and the basement level differences found in the drill site data

To verify the link between the volcanic structures and the fluid emission sites in the NW-Bohemia/Vogtland region (Fig. 1b and 1c), we have estimated their distances to each other. Figure 8a shows this relation as a histogram out to a maximum distance of 4 km, which is the cutoff for our cross-correlation. We select this maximum distance to avoid a correlation with known volcanoes at a greater distance. This correlation reveals

that 77% of all CO₂ gas emission sites (138 single site accounts) are located within less than 4 km from a Cenozoic volcanic structure. Figure 8b also supports this relation by comparing the spatial distribution of the numerous gas emission sites and the feeder dikes nearby. It is fair to note that there are springs without diatremes in the vicinity and diatremes without any indications of gas emission sites nearby.

Fig. 7 **a** Profile taken from the 3D susceptibility model crossing the main anomaly at LHB (line A–A', Fig. 5). Red line: borehole #102609. **b** The fit between the model and the measured dT for profile A–A'. The model has good correlation with the measured values with a R^2 value of around 0.8. The model thus explains most of the measured data signal

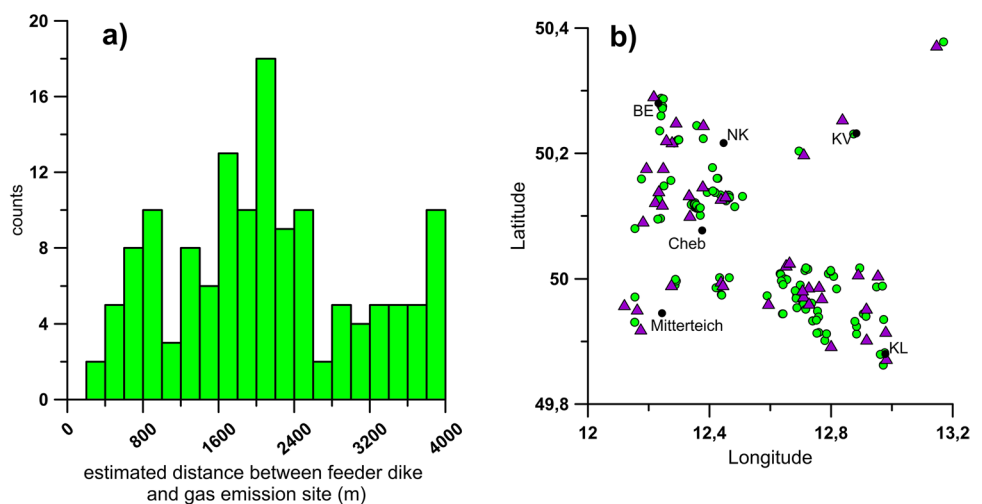


Comparison between the R_a values of 36 gas emission sites (supplement list S2) and their spatial distribution around volcanic structures indicates a decreasing R_a value with increasing distances from the volcanic structures (Fig. 9). We have restricted our analysis to an arbitrarily chosen maximum distance range of 4 km. Greater migration distances along permeable fracture zones are possible, such as along the MLFZ. However, we cannot separate if the ascent of juvenile fluids occurs along volcanically and/or tectonically controlled fracture zones at larger distances from the feeder dike.

Discussion

Our study suggests that Cenozoic magma intrusions and volcanic structures are the basis for additional fracture zones which allow the ascent of juvenile fluids to the surface. The spatial distribution of numerous Neogene and Quaternary volcanic structures (Fig. 1c) and the emission of juvenile fluids (Fig. 1b) occur mostly along an NW–SE trending zone between Bad Elster in the NW and Konstantinovy Lázně in the SE (about 25 km wide, 110 km long) and along the Eger Rift zone. Similar links had been shown to exist also at other extinct and dormant volcanic

Fig. 8 **a** Estimated distances between known volcanic structures (Fig. 1c) and CO_2 emission sites (Fig. 1b) up to a distance of 4 km and **b** spatial distribution of data presented in a). Purple triangles: basalts from Fig. 1c; green points: emission sites; black points: villages, BE: Bad Elster; NK: Nový Kostel; KV: Karlovy Vary; KL: Konstantinovy Lázně



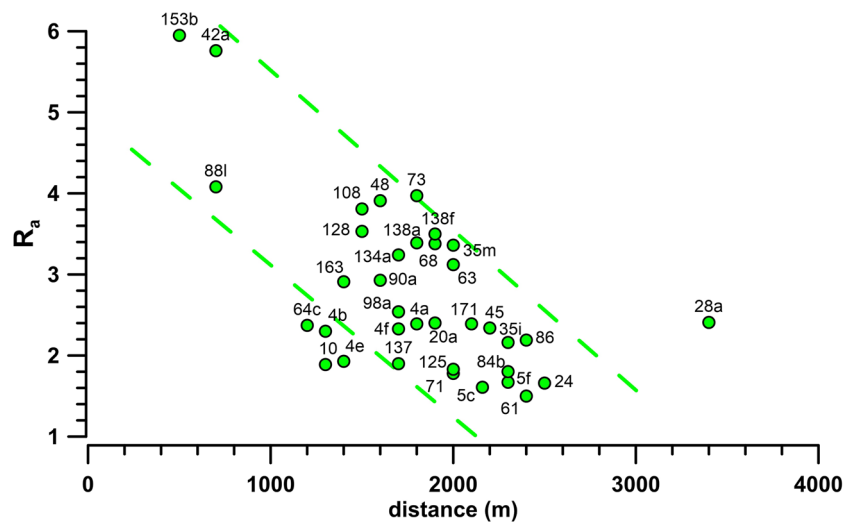


Fig. 9 Comparison of the estimated distances between the nearest known volcanic structures and the springs/mofettes with their R_a values (green points) according to the supplementary information list S2 with their references. These gas emission sites are coded by their ID

number (Heinicke and Woith 2022). The R_a values trend to decrease with increasing distances to the feeder dikes: starting from a few hundred meters (e.g., Bublák, #153b) up to 2.2 km (e.g., Bad Elster, #5f). The green dashed lines indicate a range of this trend (no correlation)

systems, as at Mt. Vulture in Italy (Caracausi et al. 2015), Rungwe Volcanic Province in Tanzania (Barry et al. 2013), Mount Onake in Japan (Sano et al. 1984), Carpathian-Pannonian Region in Romania (Kis et al. 2017), and Changbaishan volcano in China (Wei et al. 2021).

Our results suggest that the ascent of magma and fluids is controlled by the tectonic and structural properties of the basement with fracture zones, which provide transport pathways. Dikes can occupy tensile fracture zones created by extension (Gudmundsson et al. 2022; Gudmundsson and Loetveit 2005; Tamburello et al. 2018), as is the case at the Cheb basin. Dike propagation models have also suggested emplacement of dikes around the central diatreme, maar or scoria cone (cf. Rivalta et al. 2015). Buoyancy-driven fracture propagation associated with magma ascent also induces fractures at the wall rock (cf. Townsend et al. 2015). Delaney et al. (1986), for example, observed numerous joints parallel to the dike orientation, which can be used as fluid transport paths. Additionally, the dissolution processes along the wall rock due to interaction with the juvenile fluids increases the fracture permeability further (Heinicke et al. 2019). If these intrusions and fractures are associated with fault zones, as here related to subsidence within the Cheb basin, gas emission in the vicinity of diatremes or dikes is further enhanced. We consider the regional seismicity (Fig. 1b) as an important driving force to enable the continuous ongoing migration of juvenile fluids through the crust. This all means that dikes and diatremes, especially when also associated with fault zones, present permeable conduits for fluid ascent from degassing sources in the mantle.

Spatial correlation between feeder dikes and mantle helium

Highest contents of mantle-originated fluids are associated with the highest R_a values up to the upper limit of about 9 R_a for MORB and 6.3 R_a for the European subcontinental mantle helium isotope signature (Gautheron et al. 2005). This compares with a crust-derived range of about 0.02 (Ozima and Podosek 2002). The relatively fast transport up an open volcanic conduit acts as a shortcut from the upper mantle, avoiding long-term contact with the upper crust and therefore less reducing the admixture of radiogenic ^4He and loss of ^3He , which would reduce the R_a values. The opposite applies to ascent of juvenile fluids along deep-reaching fracture zones with velocities of cm to mm per year for which there is a high degree of isotope exchange (Stober 1995). The decrease in R_a with increasing distance to the source for fractures extending through upper crust has been widely observed (e.g., Barry et al. 2013; Hilton et al. 1993; Karolyt  et al. 2019; Marty et al. 1989; Sano et al. 1984; Zhang et al. 2021). These examples consider stratovolcanoes and MORB basalts and their emission of juvenile fluids at springs, mofettes, and fumaroles at distances of up to 15 km and, in one case, up to 50 km (Barry et al. 2013). R_a values decrease, for example, from about 9 R_a in the main crater area to about 4 R_a at the fluid emission sites at 15 km distance for several volcanoes in Japan (Marty et al. 1989).

In comparison to these investigations, our consideration is related to relatively small volcanic structures (dikes, diatremes) and therefore also shorter distances to the gas emission sites. We used the published R_a data of the region,

compiled in the supplementary information list S2. Figure 9 thus shows the relation between the estimated distances of the respective springs/mofettes to the closest known Cenozoic feeder dikes according to Fig. 8 and their analyzed R_a values. The relation suggests a negative trend. That is, with increasing distance to the closest feeder dike, the R_a value at the gas emission site decreases. This means that springs with R_a values greater than 1 could be supplied with juvenile fluids via a fracture system associated with these dikes. Our analysis shows only a range of estimated distances with a maximum of 4 km between dike and fluid emission site. However, longer migration distances are possible on fault zones of tectonic and structural control, but we have to consider also additional hidden volcanic structures, which could exist in the vicinity of these emission sites with increased R_a values.

The trend found in Fig. 9 thus implies that the closer the feeder dike is to the gas emission point, the higher the R_a values will be. The results suggest that tectonically weak zones, which are associated with magma ascent and dike propagation, are an important basis for the post-volcanic fluid transport along permeable fractures.

Conclusions

A link between magmatic reservoirs and juvenile fluid discharge at mineral springs and mofettes is well known, but the means of transport to the surface and why particular paths exist are much less clear. We consider feeder systems for volcanic activity in the Cenozoic as one important way that today link magmatic reservoirs at depth to surface emissions. In the NW-Bohemia/Vogtland region, Cenozoic intrusions controlled by the tectonic regime represent permeable fracture zones which allow the ascent of juvenile fluids to the surface.

Our magnetic survey of the NW Bohemia/Vogtland region resulted in the discovery of new Neogene volcanic structures which are located close to the most important juvenile fluid degassing centers of Hartoušov, Bublák/Vackovec, and Soos. Tectonic structures and associated conduits used by the Cenozoic volcanism provide conduits for the ascent and emission of juvenile fluids. Our compilation of all volcanic structures and juvenile fluid emissions for NW-Bohemia/Vogtland reveals that 77% of fluid emission sites are located less than 4 km from a volcanic structure.

Our study reveals a significant decrease in R_a values in gas emission sites with increasing distance to the volcanic structures, revealing that the location of dikes controls the location of fluid ascent.

Supplementary Information The online version contains supplementary material available at <https://doi.org/10.1007/s00445-023-01650-3>.

Acknowledgements This work is a part of a research project which was funded by the Deutsche Forschungsgemeinschaft (DFG, German Research Foundation, 285808303). We are grateful to the INGV Palermo, F. Italiano, and A. Caracausi for additional helium isotope analysis. The authors would like to thank the executive editor, A. Harris, the assistant editor, Jian-dong Xu, and the anonymous reviewer for their fruitful discussions and helpful comments.

Funding Open Access funding enabled and organized by Projekt DEAL.

Data availability The locations of the magnetic survey areas and the compiled R_a and $\delta^{13}\text{C}$ -values of the literature are available in the supplement. The comprehensive list of the CO_2 emission sites is published as an open source file by Heinicke and Woith (2022).

Open Access This article is licensed under a Creative Commons Attribution 4.0 International License, which permits use, sharing, adaptation, distribution and reproduction in any medium or format, as long as you give appropriate credit to the original author(s) and the source, provide a link to the Creative Commons licence, and indicate if changes were made. The images or other third party material in this article are included in the article's Creative Commons licence, unless indicated otherwise in a credit line to the material. If material is not included in the article's Creative Commons licence and your intended use is not permitted by statutory regulation or exceeds the permitted use, you will need to obtain permission directly from the copyright holder. To view a copy of this licence, visit <http://creativecommons.org/licenses/by/4.0/>.

References

- Abratis M, Munsel D, Viereck-Götze L (2009) Melilithite und melilithitführende magmatite des sächsischen Vogtlands: Petrographie und Mineralchemie. *Z Geol Wiss* 37:41–79
- Ackerman L, Špaček P, Magna T, Ulrych J, Svojtka M, Hegner E, Balogh K (2013) Alkaline and carbonate-rich melt metasomatism and melting of subcontinental lithospheric mantle: evidence from mantle xenoliths, NE Bavaria, Bohemian Massif. *J Petrology* 54:2597–2633. <https://doi.org/10.1093/ptrology/egt059>
- Ackerman L, Ulrych J, Randa Z, Erban V, Hegner E, Magna T, Balogh K, Frána J, Lang M, Novák JK (2015) Geochemical characteristics and petrogenesis of phonolites and trachytic rocks from the České Středohoří Volcanic Complex, the Ohře Rift, Bohemian Massif. *Lithos* 224–225:256–271. <https://doi.org/10.1016/j.lithos.2015.03.014>
- Anikiev D, Götze H-J, Meeßen C, Plonka C, Scheck-Wenderoth M, Schmidt S (2020) IGMAS+: interactive gravity and magnetic application system. <https://doi.org/10.5880/GFZ.4.5.IGMAS.V.1.3>
- Babuška V, Plomerová J (2008) Control of paths of quaternary volcanic products in western Bohemian Massif by rejuvenated Variscan triple junction of ancient microplates. *Studia Geophysica Et Geodaetica* 52:607. <https://doi.org/10.1007/s11200-008-0040-0>
- Bälz E (1908) Das Egerländer Braunkohlebecken. Glückauf 52:1830–1842
- Bankwitz P, Schneider G, Kämpf H, Bankwitz E (2003) Structural characteristics of epicentral areas in Central Europe: study case Cheb Basin (Czech Republic). *J Geodyn* 35:5–32
- Barry PH, Hilton DR, Fischer TP, de Moor JM, Mangasini F, Ramirez C (2013) Helium and carbon isotope systematics of cold “mazuku” CO_2 vents and hydrothermal gases and fluids from Rungwe Volcanic Province, southern Tanzania. *Chem Geol* 339:141–156. <https://doi.org/10.1016/j.chemgeo.2012.07.003>
- Börner R-U, Kämpf R (2019) Erstellung von bodengebundenen Karten der magnetischen Totalfeld-Anomalien -Abschlußbericht

- zum Projekt (Z 987/18), TU Bergakademie Freiberg, Institut für Geophysik und Geoinformatik
- Brandl PA, Genske FS, Beier C, Haase KM, Sprung P, Krumm SH (2015) Magmatic evidence for carbonate metasomatism in the lithospheric mantle underneath the Ohře (Eger) Rift. *J Petrol* 56:1743–1774. <https://doi.org/10.1093/ptrology/egv052>
- Bräuer K, Kämpf H, Niedermann S, Strauch G (2013) Indications for the existence of different magmatic reservoirs beneath the Eifel area (Germany): a multi-isotope (C, N, He, Ne, Ar) approach. *Chem Geol* 356:193–208. <https://doi.org/10.1016/j.chemgeo.2013.08.013>
- Bräuer K, Kämpf H, Niedermann S, Wetzel H-U (2017) Regional distribution pattern of carbon and helium isotopes from different volcanic fields in the French Massif Central: evidence for active mantle degassing and water transport. *Chem Geol* 469:4–18. <https://doi.org/10.1016/j.chemgeo.2017.04.004>
- Bräuer K, Kämpf H, Niedermann S, Strauch G (2018) Monitoring of helium and carbon isotopes in the western Eger Rift area (Czech Republic): relationships with the 2014 seismic activity and indications for recent (2000–2016) magmatic unrest. *Chem Geol* 482:131–145. <https://doi.org/10.1016/j.chemgeo.2018.02.017>
- Bräuer K, Kämpf H, Niedermann S, Strauch G, Tesař J (2008) Natural laboratory NW Bohemia: comprehensive fluid studies between 1992 and 2005 used to trace geodynamic processes. *Geochem Geophys Geosyst* 9. <https://doi.org/10.1029/2007gc001921>
- Bräuer K, Kämpf H, Strauch G (2014) Seismically triggered anomalies in the isotope signatures of mantle-derived gases detected at degassing sites along two neighboring faults in NW Bohemia, central Europe. *J Geophys Res* 119. <https://doi.org/10.1002/2014jb011044>
- Bucha V, Horacek J, Malkovsky M (1990) Paleomagnetic stratigraphy of the Tertiary of the Cheb basin (W Bohemia). *Věstník Ústředního ústavu geologického* 5:267–278
- Büchner J, Tietz O, Viereck L, Suhr P, Abratis M (2015) Volcanology, geochemistry and age of the Lausitz Volcanic Field. *Int J Earth Sci* 104:2057–2083. <https://doi.org/10.1007/s00531-015-1165-3>
- Buck WR, Lavier LL, Poliakov ANB (2005) Modes of faulting at mid-ocean ridges. *Nature* 434:719–723. <https://doi.org/10.1038/nature03358>
- Burda J, Baburek J (1998) Hydrologie des westböhmisches Bäderdreieckes. *Jber Mitt Oberrhein Geol Ver* 80:91–110
- Cajz V, Rapprich V, Erban V, Pécskay Z, Radoň M (2009) Late Miocene volcanic activity in the České středohoří Mountains (Ohře/Eger Graben, northern Bohemia). *Geologica Carpathica* 60:519–533. <https://doi.org/10.2478/v10096-009-0038-8>
- Caracausi A, Sulli A (2019) Outgassing of mantle volatiles in compressional tectonic regime away from volcanism: the role of continental delamination. *Geochem Geophys Geosyst* 20:2007–2020. <https://doi.org/10.1029/2018GC008046>
- Caracausi A, Paternoster M, Nuccio PM (2015) Mantle CO₂ degassing at Mt. Vulture volcano (Italy): relationship between CO₂ outgassing of volcanoes and the time of their last eruption. *Earth Planet Sci Lett* 411:268–280. <https://doi.org/10.1016/j.epsl.2014.11.049>
- Carlé W (1958) Kohlensäure, Erdwärme und Herdlage im Uracher Vulkangebiet und seiner weiteren Umgebung. *Z Dt Geol Ges* 110:71–101. <https://doi.org/10.1127/zdgg/110/1958/71>
- Carlé W (1975) Die Mineral- und Thermalwässer von Mitteleuropa: Geologie, Chemismus, Genese. Bücher der Z Naturwiss Rundschau. Wiss. Verl.-Ges, Stuttgart
- Cháb J, Stráník Z, Eliáš M (2007) Geologická mapa České republiky, 1st edn. Česká Geolog. Služba, Praha
- Chadima M, Cajz V, Týcová P (2009) On the interpretation of normal and inverse magnetic fabric in dikes: examples from the Eger Graben, NW Bohemian Massif. *Tectonophysics* 466:47–63. <https://doi.org/10.1016/j.tecto.2008.09.005>
- Chiodini G, Granieri D, Avino R, Caliro S, Costa A, Minopoli C, Vilardo G (2010) Non-volcanic CO₂ Earth degassing: case of Mefite d'Ansanto (southern Apennines), Italy. *Geophys Res Lett* 37:1–4. <https://doi.org/10.1029/2010GL042858>
- Clauser C, Griesshaber E, Neugebauer HJ (2002) Decoupled thermal and mantle helium anomalies: implications for the transport regime in continental rift zones. *J Geophys Res* 107:ETG 1–16. <https://doi.org/10.1029/2001JB000675>
- Dahm T, Fischer T, Hainzl S (2008) Mechanical intrusion models and their implications for the possibility of magma-driven swarms in NW Bohemia Region. *Studia Geophysica Et Geodaetica* 52:529–548. <https://doi.org/10.1007/s11200-008-0036-9>
- Dahm T, Heimann S, Funke S, Wendt S, Rappsilber I, Bindi D, Plenefisch T, Cotton F (2018) Seismicity in the block mountains between Halle and Leipzig, Central Germany: centroid moment tensors, ground motion simulation, and felt intensities of two M ≈ 3 earthquakes in 2015 and 2017. *J Seismolog* 22:985–1003. <https://doi.org/10.1007/s10950-018-9746-9>
- Dahm T, Stiller M, Mechie J, Heimann S, Hensch M, Woith H, Schmidt B, Gabriel G, Weber M (2020) Seismological and geophysical signatures of the deep crustal magma systems of the Cenozoic volcanic fields beneath the Eifel, Germany. *Geochem Geophys Geosyst* 21:1–21. <https://doi.org/10.1029/2020GC009062>
- Delaney PT, Pollard DD, Ziony JI, McKee EH (1986) Field relations between dikes and joints: emplacement processes and paleostress analysis. *J Geophys Res* 91:4920. <https://doi.org/10.1029/JB091iB05p04920>
- Dietl A (1942) Die Säuerlinge des Egerlandes. *Der Balneologe* 9:269–284
- Dobeš M, Herzog F, Mazač O (1986) Die geophysikalische Untersuchung der hydrogeologischen Strukturen im Cheb-Becken. *J Geol Sci - Appl Geophys*:117–158
- Dupalová T, Sracek O, Vencelides Z, Žák K (2012) The origin of thermal waters in the northeastern part of the Eger Rift, Czech Republic. *Appl Geochem* 27:689–702. <https://doi.org/10.1016/j.apgeochem.2011.11.016>
- Egerter H-G, Plötner G, Dvořák J, Jordan H (1984) Geochemische Beziehungen in vogtländisch-westböhmisches Mineralwässern. *Abh. Sächs. Akad. Wiss. Leipzig, math.-nat. Kl* 56:1–60
- Emmert U, v. Horstig G, Stettner G (2007) General geological map of the Federal Republic of Germany - CC 6334 Bayreuth: GÜK200 - CC 6334 Bayreuth. Bundesanstalt für Geowissenschaften und Rohstoffe, Hannover
- Fischer TP (2008) Fluxes of volatiles (H₂O, CO₂, N₂, Cl, F) from arc volcanoes. *Geochem J* 42:21–38. <https://doi.org/10.2343/geochemj.42.21>
- Fischer T, Horálek J, Hrubcová P, Vavryčuk V, Bräuer K, Kämpf H (2014) Intra-continental earthquake swarms in West-Bohemia and Vogtland: a review. *Tectonophysics* 611:1–27. <https://doi.org/10.1016/j.tecto.2013.11.001>
- Flechsig C, Heinicke J, Mrlina J, Kämpf H, Nickschick T, Schmidt A, Bayer T, Günther T, Rucker C, Seidel E, Seidl M (2015) Integrated geophysical and geological methods to investigate the inner and outer structures of the Quaternary Mytina maar (W-Bohemia, Czech Republic). *Int J Earth Sci* 104:2087–2105. <https://doi.org/10.1007/s00531-014-1136-0>
- Gautheron C, Moreira M, Allègre C (2005) He, Ne and Ar composition of the European lithospheric mantle. *Chem Geol* 217:97–112. <https://doi.org/10.1016/j.chemgeo.2004.12.009>
- Geissler WH, Kämpf H, Kind R, Bräuer K, Klinge K, Plenefisch T, Horálek J, Zednik J, Nehybka V (2005) Seismic structure and location of a CO₂ source in the upper mantle of the western Eger (Ohre) Rift, central Europe. *Tectonics* 24:1–25. <https://doi.org/10.1029/2004tc001672>
- Götze H-J, Lahmeyer B (1988) Application of three-dimensional interactive modeling in gravity and magnetics. *Geophysics* 53:1096–1108. <https://doi.org/10.1190/1.1442546>

- Griesshaber E, O'Nions RK, Oxburgh ER (1992) Helium and carbon isotope systematics in crustal fluids from the Eifel, the Rhine Graben and Black Forest, F.R.G. *Chem Geol* 99:213–235. [https://doi.org/10.1016/0009-2541\(92\)90178-8](https://doi.org/10.1016/0009-2541(92)90178-8)
- Gudmundsson A, Loetveit IF (2005) Dyke emplacement in a layered and faulted rift zone. *J Volcanol Geoth Res* 144:311–327. <https://doi.org/10.1016/j.jvolgeores.2004.11.027>
- Gudmundsson A, Drymoni K, Browning J, Acocella V, Amelung F, Bonali FL, Elshaafi A, Galindo I, Geshi N, Geyer A, Heap MJ, Karaoglu Ö, Kusumoto S, Marti J, Pinel V, Tibaldi A, Thordarson T, Walter TR (2022) Volcanotectonics: the tectonics and physics of volcanoes and their eruption mechanics. *Bull Volcanol* 84:1–8. <https://doi.org/10.1007/s00445-022-01582-4>
- Hecht L, Vignerresse JL, Morteani G (1997) Constraints on the origin of zonation of the granite complexes in the Fichtelgebirge (Germany and Czech Republic) evidence from a gravity and geochemical study. *Geol Rundschau* 86:S93–S109. <https://doi.org/10.1007/pl00014669>
- Heidbach O, Rajabi M, Cui X, Fuchs K, Müller B, Reinecker J, Reiter K, Tingay M, Wenzel F, Xie F, Ziegler MO, Zoback M-L, Zoback M (2018) The World Stress Map database release 2016: crustal stress pattern across scales. *Tectonophys* 744:484–498. <https://doi.org/10.1016/j.tecto.2018.07.007>
- Heinicke J, Woith H (2022) Mofettes and CO₂-rich mineral waters of the NW Bohemia-Vogtland region. *GFZ Data Services*. <https://doi.org/10.5880/figdeo.2022.036>
- Heinicke J, Stephan T, Alexandrakis C, Gaupp R, Buske S (2019) Alteration as possible cause for transition from brittle failure to aseismic slip: the case of the NW-Bohemia/Vogtland earthquake swarm region. *J Geodyn* 124:79–92. <https://doi.org/10.1016/j.jog.2019.01.010>
- Heinicke J, Braun T, Alexandrakis-Zieger C, Buske S (2022) Possible origin of the spatiotemporal evolution of the 2008 earthquake swarm in Northwest-Bohemia Czech Republic. *Phys Earth Planet Inter* 333:106941. <https://doi.org/10.1016/j.pepi.2022.106941>
- Hilton DR, Hammerschmidt K, Teufel S, Friedrichsen H (1993) Helium isotope characteristics of Andean geothermal fluids and lavas. *Earth Planet Sci Lett* 120:265–282. [https://doi.org/10.1016/0012-821X\(93\)90244-4](https://doi.org/10.1016/0012-821X(93)90244-4)
- Horálek J, Hampl F, Boušková A, Fischer T (1996) Seismic regime of the west Bohemian earthquake swarm region: preliminary results. *Studia Geophysica Et Geodaetica* 40:398–412. <https://doi.org/10.1007/bf02300767>
- Hoth K, Tischendorf G, Berger HJ (1981) Geologische Karte Erzgebirge/Vogtland. Sächsisches Landesamt für Umwelt und Geologie
- Hrubcová P, Geissler WH, Bräuer K, Vavryčuk V, Tomek Č, Kämpf H (2017) Active magmatic underplating in western Eger Rift, central Europe. *Tectonics* 36. <https://doi.org/10.1002/2017tc004710>
- Hunt JA, Zafu A, Mather A, Pyle DM, Barry PH (2017) Spatially variable CO₂ degassing in the main Ethiopian Rift: implications for magma storage, volatile transport, and rift-related emissions. *Geochem Geophys Geosyst* 18:3714–3737. <https://doi.org/10.1002/2017GC006975>
- Jahnel F (1937) Mineralquellen und Gasquellen im Egerer Landschaftsgebiet. Unser Egerland - Schriftenreihe für lebendige Heimatpflege 41:90–102
- Kämpf H, Broge AS, Marzban P, Allahbakhshi M, Nickschick T (2019) Nonvolcanic carbon dioxide emission at continental rifts: the Bublak Mofette area, western Eger Rift, Czech Republic. *Geofluids* 2019:1–19. <https://doi.org/10.1155/2019/4852706>
- Karolytė R, Johnson G, Györe D, Serno S, Flude S, Stuart FM, Chivas AR, Boyce A, Gilfillan SM (2019) Tracing the migration of mantle CO₂ in gas fields and mineral water springs in southeast Australia using noble gas and stable isotopes. *Geochim Cosmochim Acta* 259:109–128. <https://doi.org/10.1016/j.gca.2019.06.002>
- Kennedy BM, van Soest MC (2007) Flow of mantle fluids through the ductile lower crust: helium isotope trends. *Science* 318:1433–1436. <https://doi.org/10.1126/science.1147537>
- Kis B-M, Ionescu A, Cardellini C, Harangi S, Baciu C, Caracausi A, Viveiros F (2017) Quantification of carbon dioxide emissions of Ciomadul, the youngest volcano of the Carpathian-Pannonian region (eastern-central Europe, Romania). *J Volcanol Geoth Res* 341:119–130. <https://doi.org/10.1016/j.jvolgeores.2017.05.025>
- Korn M, Funke S, Wendt S (2008) Seismicity and seismotectonics of west Saxony, Germany: new insights from recent seismicity observed with the Saxonian seismic network. *Studia Geophysica Et Geodaetica* 52:479–492. <https://doi.org/10.1007/s11200-008-0033-z>
- Kroner U, Hahn T, Romer RL, Linnemann U (2007) The Variscan orogeny in the Saxo-Thuringian zone — heterogenous overprint of Cadomian/Paleozoic Peri-Gondwana crust. *Geol Soc Am Spec Pap* 423:153–172. [https://doi.org/10.1130/2007.2423\(06\)](https://doi.org/10.1130/2007.2423(06))
- Kulongoski JT, Hilton DR, Barry PH, Esser BK, Hillemonds D, Belitz K (2013) Volatile fluxes through the Big Bend section of the San Andreas Fault, California: Helium and carbon-dioxide systematics. *Chem Geol* 339:92–102. <https://doi.org/10.1016/j.chemgeo.2012.09.007>
- Lindner H, Gabriel G, Götze H-J, Käppler R, Suhr P (2006) Geophysical and geological investigation of maar structures in the Upper Lusatia region (East Saxony). *Z Deut Geol Ges* 157:355–372. <https://doi.org/10.1127/1860-1804/2006/0157-0355>
- Lorenz V (2007) Syn- and post-eruptive hazards of maar-diatreme volcanoes. *J Volcanol Geoth Res* 159:285–312. <https://doi.org/10.1016/j.jvolgeores.2006.02.015>
- Marty B, Jambon A, Sano Y (1989) Helium isotopes and CO₂ in volcanic gases of Japan. *Chem Geol* 76:25–40. [https://doi.org/10.1016/0009-2541\(89\)90125-3](https://doi.org/10.1016/0009-2541(89)90125-3)
- Mlčoch B, Skácelová Z (2009) Digital elevation model of the crystalline basement of the Cheb and Sokolov Basin areas (western Bohemia, central Europe). *Z Geol Wiss* 37:145–152
- Mrlina J, Kämpf H, Geissler WH, van den Bogaard (2007) Assumed quaternary maar structure at the Czech/German border between Mýtina and Neualbenreuth (western Eger Rift, central Europe): geophysical, petrochemical and geochronological indications. *Z Geol Wiss* 35:213–230
- Mrlina J, Kämpf H, Kroner C, Mingram J, Stebich M, Brauer A, Geissler WH, Kallmeyer J, Matthes H, Seidl M (2009) Discovery of the first quaternary maar in the Bohemian Massif, central Europe, based on combined geophysical and geological surveys. *J Volcanol Geoth Res* 182:97–112. <https://doi.org/10.1016/j.jvolgeores.2009.01.027>
- Ozima M, Podosek FA (2002) Noble gas geochemistry, 2nd edn. Cambridge University Press, Cambridge, New York
- Pearce J, Czernichowski-Lauriol I, Lombardi S, Brune S, Nador A, Baker J, Pauwels H, Hatziyannis G, Beaubien S, Faber E (2004) A review of natural CO₂ accumulations in Europe as analogues for geological sequestration. *Geol Soc London, Special Publications* 233:29–41. <https://doi.org/10.1144/GSL.SP.2004.233.01.04>
- Perez NM, Hernandez PA, Padilla G, Nolasco D, Barrancos J, Melian G, Padron E, Dionis S, Calvo D, Rodriguez F, Notsu K, Mori T, Kusakabe M, Arpa MC, Reniva P, Ibarra M (2011) Global CO₂ emission from volcanic lakes. *Geol* 39:235–238. <https://doi.org/10.1130/G31586.1>
- Pešek J, Brož B, Brzobohatý R, Dašková J, Doláková N, Elznic A, Fejfar O, Franců J, Hladilová Š, Holcová K, Honěk J, Hoňková K, Kvaček J, Kvaček Z, Macůrek V, Mikuláš R, Opluštil S, Rojčík P, Spudil J, Svobodová M, Sýkorová I, Švábenická L, Teodoridis V,

- Tomanová-Petrová P (2014) Tertiary basins and lignite deposits of the Czech Republic. Czech Geol Survey, Prague
- Petek A, Reuther C-D, Schunk R (2011) Neotectonic evolution of the Cheb Basin (Northwestern Bohemia, Czech Republic) and its implications for the late Pliocene to recent crustal deformation in the western part of the Eger Rift. *Z Geol Wiss* 39:335–365
- Pitra P, Burg J-P, Guiraud M (1999) Late Variscan strike-slip tectonics between the Tepla-Barrandian and Moldanubian terranes (Czech Bohemian Massif): petrostructural evidence. *J Geol Soc* 156:1003–1020. <https://doi.org/10.1144/gsjgs.156.5.1003>
- Pohl D, Wetzel H-U, Grünthal G (2006) Tektonische Untersuchungen im Raum Vogtland-Leipzig mit Hilfe der Fernerkundung - Vortrag bei der 26. Wiss - Techn Jahrestagung der DGPF, Berlin. Geoinformatik und Erderkundung (DGPF):277–286
- Rivalta E, Taisne B, Bungler AP, Katz RF (2015) A review of mechanical models of dike propagation: schools of thought, results and future directions. *Tectonophysics* 638:1–42. <https://doi.org/10.1016/j.tecto.2014.10.003>
- Rohrmüller J, Horn P, Peterek A, Teipel U (2005) Geology and structure of the lithosphere. Schriftenreihe der DGG - Exkursionsführer GeoErlangen 40:46–50
- Sano Y, Nakamura Y, Wakita H, Urabe A, Tominaga T (1984) Helium-3 emission related to volcanic activity. *Science* 224:150–151. <https://doi.org/10.1126/science.224.4645.150>
- Skácelová Z, Rappich V, Valenta J, Hartvich F, Šrámek J, Radoň M, Gaždová R, Nováková L, Kolínský P, Pécskay Z (2012) Geophysical research on structure of partly eroded maar volcanoes: Miocene Hnojnice and Oligocene Rychnov volcanoes (northern Czech Republic). *Bull. Geosci.* 333–345. <https://doi.org/10.3190/jgeosci.072>
- Sonnabend L (2022) Neotektonik und Seismizität in Westsachsen und Nordwestböhmen. Dissertation, Universität Leipzig
- Sorey ML, Evans WC, Kennedy BM, Farrar CD, Hainsworth LJ, Hausback B (1998) Carbon dioxide and helium emissions from a reservoir of magmatic gas beneath Mammoth Mountain, California. *J Geophys Res* 103:15303–15323
- Špičák A, Horálek J, Babuška A, Tomek C, Vanek J (1999) Magma intrusions and earthquake swarm occurrence in the western part of the Bohemian Massif. *Studia Geophysica Et Geodaetica* 43:87–106
- Špičáková L, Uličný D, Koudelková G (2000) Tectonosedimentary evolution of the Cheb basin (NW Bohemia, Czech Republic) between Late Oligocene and Pliocene: a preliminary note. *Studia Geophysica Et Geodaetica* 44:556–580. <https://doi.org/10.1023/a:1021819802569>
- Springorum KA (2000) The Cheb basin and the mineral springs of the Františkovy Lázně (Franzensbad), Czech Republic. Master Thesis, Rheinisch-Westfälische Techn Hochschule Aachen and Charles University Prague
- Stober I (1995) Die Wasserführung des kristallinen Grundgebirges, Stuttgart
- Storch Kv (1998) Herkunft der balneologisch wertbestimmenden Eigenschaften in sächsischen Mineral- und Thermalwässern. UFZ-Report, 24/1998
- Tamburello G, Pondrelli S, Chiadini G, Rouwet D (2018) Global-scale control of extensional tectonics on CO₂ earth degassing. *Nat Commun* 9:4608. <https://doi.org/10.1038/s41467-018-07087-z>
- Tang Q, Zhang M, Li C, Yu M, Li L (2013) The chemical compositions and abundances of volatiles in the Siberian large igneous province: constraints on magmatic CO₂ and SO₂ emissions into the atmosphere. *Chem Geol* 339:84–91. <https://doi.org/10.1016/j.chemgeo.2012.08.031>
- Townsend M, Pollard DD, Johnson K, Culha C (2015) Jointing around magmatic dikes as a precursor to the development of volcanic plugs. *Bull Volcanol* 77. <https://doi.org/10.1007/s00445-015-0978-z>
- Ulrych J, Lloyd FE, Balogh K (2003) Age relations and geochemical constraints of Cenozoic alkaline volcanic series in W Bohemia: a review. *Geolines* 15:168–180
- Ulrych J, Dostal J, Adamovic J, Jelinek E, Spacek P, Hegner E, Balogh K (2011) Recurrent Cenozoic volcanic activity in the Bohemian Massif (Czech Republic). *Lithos* 123:133–144. <https://doi.org/10.1016/j.lithos.2010.12.008>
- Ulrych J, Krmíček L, Tomek Č, Lloyd FE, Ladenberger A, Ackerman L, Balogh K (2016) Petrogenesis of Miocene alkaline volcanic suites from western Bohemia: whole rock geochemistry and Sr–Nd–Pb isotopic signatures. *Geochem* 76:77–93. <https://doi.org/10.1016/j.chemer.2015.11.003>
- Vavryčuk V, Adamová P, Doubravová J, Ren Y (2021) Mapping stress and fluids on faults by nonshear earthquakes. *J Geophys Res* 126. <https://doi.org/10.1029/2020JB021287>
- Vavryčuk V, Hrubcová P (2017) Seismological evidence of fault weakening due to erosion by fluids from observations of intraplate earthquake swarms. *J Geophys Res* 122:3701–3718. <https://doi.org/10.1002/2017jb013958>
- Wei F, Xu J, Kong Q, Liu S, Xu D, Pan B (2021) Sources of CH₄ with variable carbon isotopes from Changbaishan volcano in NE China: implications for the feeding system. *J Volcanol Geoth Res* 419:107355. <https://doi.org/10.1016/j.jvolgeores.2021.107355>
- Weinlich FH, Bräuer K, Kämpf H, Strauch G, Tesar J, Weise SM (1999) An active subcontinental mantle volatile system in the western Eger rift, central Europe: gas flux, isotopic (He, C, and N) and compositional fingerprints. *Geochim Cosmochim Acta* 63:3653–3671
- Weinlich FH, Bräuer K, Kämpf H, Strauch G, Tesar J, Weise SM (2003) Gas flux and tectonic structure in the western Eger Rift, Karlovy Vary - Oberpfalz and Oberfranken, Bavaria. *Geolines* 15:181–187
- White J, Ross P-S (2011) Maar-diatreme volcanoes: a review. *J Volcanol Geoth Res* 201:1–29. <https://doi.org/10.1016/j.jvolgeores.2011.01.010>
- Zhang M, Xu S, Zhou X, Caracausi A, Sano Y, Guo Z, Zheng G, Lang Y-C, Liu C-Q (2021) Deciphering a mantle degassing transect related with India-Asia continental convergence from the perspective of volatile origin and outgassing. *Geochim Cosmochim Acta* 310:61–78. <https://doi.org/10.1016/j.gca.2021.07.010>